CILAMCE 2017
Florianópolis - Santa Catarina - Brazil

OBSERVATION OF THE SOMMERFELD EFFECT IN WIND TURBINE TOWERS

Bruno Roberto Ferreira

Reyolando Manoel Lopes Rebello da Fonseca Brasil

bruno.roberto@aluno.ufabc.edu.br

reyolando.brasil@ufabc.edu.br

Universidade Federal do ABC (UFBAC)

Alameda da Universidade, São Bernardo do Campo, Anchieta, 09606-045, SP, Brazil

Abstract. *In this work, the vibrations of wind turbine tower modeled as a nonlinear one degree of freedom structural system excited by a non-ideal power supply are studied and analyzed while investigating specifics behaviors predicted by the literature. The equations of motion were obtained by Lagrange's formulation, and afterwards its numerical solutions were obtained. Some key parameters of the oscillation study, as the natural frequency of the system, were obtained using the Rayleigh method. One parameter that was found to be specifically related to the observation of the phenomena was the eccentricity of the unbalanced mass of the power supply, related and defined in this work by the level of balance quality of the rotor. From the observation of the resonance curves and response from the system's motion obtained it was possible to observe the Sommerfeld effect, comparing the results with the ones obtained in the literature of similar cases.*

Keywords: *Sommerfeld effect, Wind turbine, Nonlinear oscillations, Non-ideal power supply.*

INTRODUCTION

Discontinuities and "jumps" have been observed in Oscillation Theory studies. These phenomena in the dynamic behavior are especially seen when the structure interacts with an oscillating energy source. One case of this, discussed by Kononenko (1969), is a nonlinear system excited by a non-ideal power supply, in which is possible to observe these "jumps" in the resonance curve of the system, called Sommerfeld effect.

A system consisted by a wind turbine tower and rotor is very likely to present these phenomena, specially due to the considerable height of these towers, which reflects on its mechanical proprieties, making the observation more apparent. Having this system in mind, this work intends to verify the interaction between a power supply and the structure, pointing out and analyzing the discontinuities that may outcome in these oscillations.

A one degree of freedom model was utilized to represent the system, and the equations of motion were obtained by Lagrange's formulation. Afterwards, its numerical solutions were obtained. Some key parameters of the oscillation study, as the natural frequency of the system, were obtained using the Rayleigh method.

1 METHODS FOR DYNAMICAL ANALYSIS

In this session, the methods used to obtain the equations of motion of the coupled oscillation resulting from the interaction of the tower structure with the power supply (or turbine, in this case) are discussed.

1.1 Model of the system

As stated before, the system composed by the wind turbine tower and its rotor was modelled as a one degree of freedom system, composed by a cantilever beam with a non-ideal power supply mounted at its free end, as described in Figs. 1 and 2.

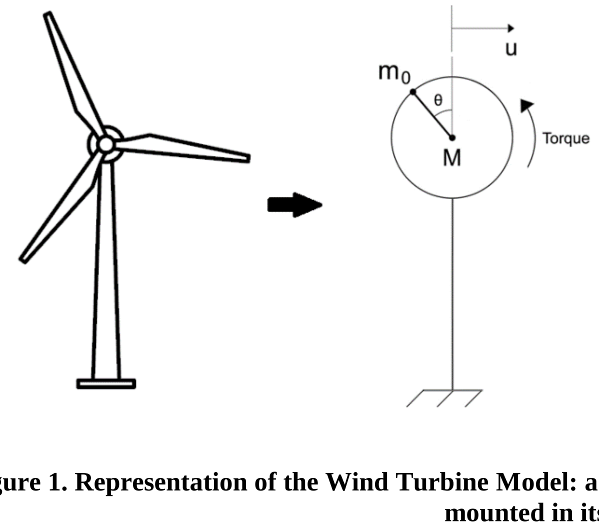

Figure 1. Representation of the Wind Turbine Model: a cantilever beam with a non-ideal power supply mounted in its top.

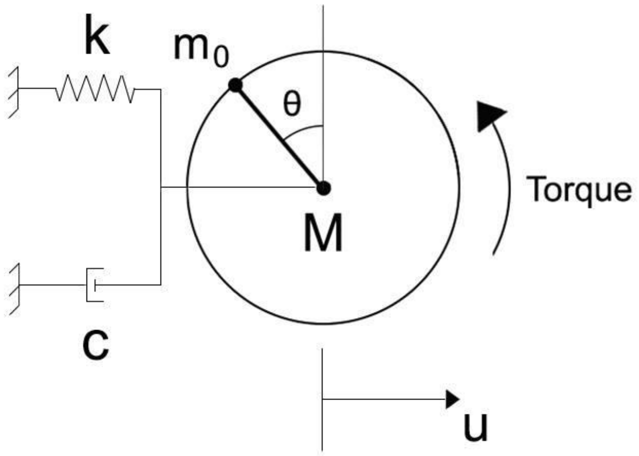

Figure 2. Model representing the cantilever beam as a combination of a spring and damper.

It is important to notice that despite the beam presenting motion in the horizontal axis only, the model described in Figs. 1 and 2 has 2 degrees of freedom, u and θ. This is a characteristic of nonlinear systems.

1.2 Lagrange's Formulation

Before beginning the formulation, the boundary conditions considered for the system presented in Fig. 2 are described in (1)

$$\begin{cases} x_M = u \\ y_M = 0 \\ \dot{x_M} = \dot{u} \\ \dot{y_M} = 0 \end{cases} \tag{1}$$

Where *x* is the horizontal and *y* the vertical axis mtion. The initial state of motion is described by the system of equations (2)

$$\begin{cases} y_0 = \ e\cos(\theta) \\ x_0 = \ u - e\sin(\theta) \\ \dot{y_0} = \ -\dot{\theta} e\sin(\theta) \\ \dot{x_0} = \ \dot{u} - \dot{\theta} e\cos(\theta) \end{cases} \tag{2}$$

where *e* represents the eccentricity of the power supply, i.e. radius of the unbalanced mass m_0.

The kinetics Energy of the system (*T*) can be seen in (3)

$$T = \frac{1}{2}[M\dot{u}^2 + J\dot{\theta}^2 + m_0(\dot{\theta}^2 e^2 + \ \dot{u}^2 - 2\dot{u}\dot{\theta} e\cos(\theta))] \tag{3}$$

where *J* (the moment of inertia of the rotor), *M* and m_0 are parameters of the rotor, in this study, obtained from the ACCIONA® AW3000 catalog, which was selected for its wide applicability in onshore concrete tower wind turbines.

The potential energy (V) of the system is expressed by (4)

$$V = \frac{1}{2}ku^2 \tag{4}$$

Applying the first type Lagrange equations (5)

$$N_i = \frac{d}{dt}\left(\frac{\partial T}{\partial \dot{q}_i}\right) - \frac{\partial T}{\partial q_i} + \frac{\partial V}{\partial q_i} \tag{5}$$

for

- $i=1$: u degree of freedom; $N_1 = -c \cdot \dot{u}$
- $i=2$: θ degree of freedom; $N_2 = \mathcal{L}(\dot{\theta}) - \mathcal{H}(\dot{\theta})$, which corresponds to the torque subtracted by the losses of the rotor.

The equations of motion of the system (6) are obtained.

$$\begin{cases} (\boldsymbol{M} + \boldsymbol{m_0})\ddot{\boldsymbol{u}} + \boldsymbol{c}\dot{\boldsymbol{u}} + \boldsymbol{k}\boldsymbol{u} = \boldsymbol{m_0}\boldsymbol{e}\left[\ddot{\boldsymbol{\theta}}\cos(\boldsymbol{\theta}) - \dot{\boldsymbol{\theta}}^2\sin(\boldsymbol{\theta})\right] \\ \boldsymbol{\mathcal{L}}(\dot{\boldsymbol{\theta}}) - \boldsymbol{\mathcal{H}}(\dot{\boldsymbol{\theta}}) = (\boldsymbol{J} + \boldsymbol{m_0}\boldsymbol{e}^2)\ddot{\boldsymbol{\theta}} - \boldsymbol{m_0}\ddot{\boldsymbol{u}}\boldsymbol{e}\cos(\boldsymbol{\theta}) \end{cases} \tag{6}$$

From the system of equations (6), the motion of the system is coupled, with the motion u depending on θ and vice-versa.

1.3 Rayleigh Method for Tower Parameters Determination

In order to determine the parameters of the system M^* (equivalent mass), k (stiffness coefficient), c (damping coefficient) and ω (natural frequency), we apply to the tower Rayleigh's method, with a shape function defined by (7).

$$\phi(u) = 1 - \cos\left(\frac{\pi}{2L}u\right) \tag{7}$$

where L is the height of the tower.

With this shape function, it was possible to obtain the parameters defined by the Rayleigh method in (8), (9) and (10).

$$M^* = \int_0^L \rho A \varphi^2(u)du \tag{8}$$

$$k^* = \int_0^L EI{\varphi''}^2(u)du \tag{9}$$

$$\omega = \sqrt{k^*/M} \tag{10}$$

where E is the Elastic modulus, ρ is the density of the concrete (2450 kg/m^3), I the moment of Inertia and A is the cross section of the tower.

2 NON-IDEAL POWER SUPPLY

In ideal cases, a power supply provides energy for the oscillating system without interaction between them. However, when the motion of the system interacts with the rotor, i.e. the power supply rotor motion is affected by the structure motion as well as the structure is affected by the rotor, then the system is classified as non-ideal.

According to Simons (2008), the resonance curve of a system can be calculated by (11).

$$\mathrm{E}(\dot{\theta}) = \frac{\mathrm{c}}{2\dot{\theta}}\omega^2\mathrm{R}^2 \tag{11}$$

$$\mathrm{R} = \frac{\mathrm{m_0 e}\dot{\theta}^2}{\mathrm{k}}\mathrm{D} \tag{12}$$

$$D = \frac{1}{\left(\sqrt{((1-\beta^2)^2 + (2\zeta\beta)^2)}\right)} \tag{13}$$

$$\beta = \frac{\dot{\theta}}{\omega} \tag{14}$$

In the study of the stability of systems powered by non-ideal generators it is important to consider the curves that represent the power supply torque: the generator characteristic curve ($L(\dot{\theta})$), and the losses due to internal resistances of the rotor curve ($H(\dot{\theta})$).

According to Kononeko (1969), the stability state of systems as the one studied in this work occur at the intersection of the Curve of Total energy consumed by the structure ($\mathrm{S}(\dot{\theta})$) – given by adding up $E(\dot{\theta})$ and $H(\dot{\theta})$ – and $L(\dot{\theta})$. This point represents the stability state between the energies provided ($L(\dot{\theta})$) and consumed ($\mathrm{S}(\dot{\theta})$) by the system, which can be classified as stable if the curves that meet present opposite signal derivatives or unstable otherwise.

It is worth to note that the damping ratio (ζ) considered was 0.1, or 10%, which is quite large for concrete structures.

3 SOMMERFELD EFFECT

Analyzing Kononenko's (1969) experiment, where one can see an electric motor positioned on the free end of a cantilever beam, it is possible to observe the response of a non-ideal power supply when a certain characteristic curve is given. It could be represented by Fig. 3.

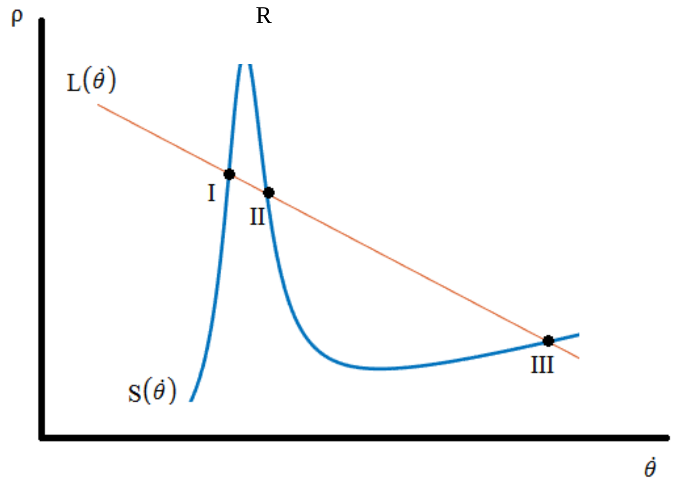

Figure 3. Total Energy Consumed by the System Curve (S) and characteristic curve (L)

In Fi. 3, when considering the increasing case (case when the system is increasing its rotor's angular velocity) it is possible to notice that the curves can meet at three different points. The stability point is given by I, an stable point because the L and S curves have opposite directions. Still in the crescent case, II could be classified as unstable and III as stable.

When observing the results of the Kononenko practical experiment, one can see discontinuities where the curves are considered unstable. These discontinuities are called the Sommerfeld Effect.

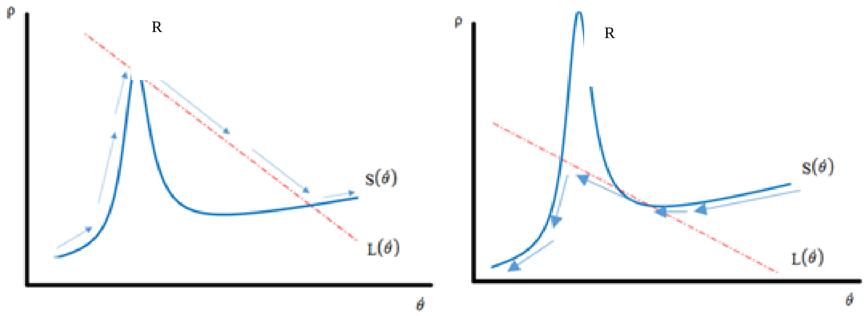

Figure 4. Boundary Characteristics for the increasing (left) and decreasing (right) cases

In Fig. 4 it is possible to observe the discontinuities for both increasing and decreasing cases, where all the S curve region not marked by arrows would not be visible in a practical experiment.

4 SIMULATION

4.1 Input Characteristics of the System

For the simulation, it were considered 3 different cases of balance quality degree, according to ISO 1940/1, G2.5 (Generator Rotor – ideal for wind turbines), G16 and G40. Important to notice that the G 16 and G 40 cases were picked in order to see how this parameter affects the system.

For the turbine tower, it was considered the model studied by Quilligan, O'Connor e Pakrashi (2012), for being compatible with the ACCIONA® AW3000 turbine selected for the study. The curves L and H are not provided in the catalog and were constructed for each balance quality degree in order to be able to observe the Sommerfeld Effect.

Table 1. Wind Turbine Tower Structure Characteristics.

Tower Structure Proprieties	
Tower Height	103m
Base Diameter	8.2m
Tip Diameter	4.8m
Concrete thickness	0.25m
Damping Ratio (ζ)	10%

Table 2. Common Characteristics for the different cases of balance quality degree.

Common Characteristics	
ω [rad/s]	2.650
c [10^3·Ns/m]	205
M [10^3·kg]*	243
ρ [kg/m^3]	2450
J [10^6.kg.m^2]	87.9
k [10^6.N/m]	2.715

Table 3. Particular Characteristics for the different cases of balance quality degree.

Particular Characteristics	G 2.5	G 16	G 40
e [mm]	1.8	11.6	28.9
$L(\dot{\theta})$	$8000\text{-}1250\dot{\theta}$	$(12\text{-}2\cdot\dot{\theta})\cdot 10^6$	$(4.5\text{-}0.5\cdot\dot{\theta})10^8$
$H(\dot{\theta})$	$250\cdot\dot{\theta}$	$10^6\cdot\dot{\theta}$	$0.5\cdot 10^8\cdot\dot{\theta}$

Using the characteristics presented in tables 1, 2 and 3, it is possible to plot Energy and Characteristic Curves of the Systems against angular velocity of the rotor, showed in Figure 5.

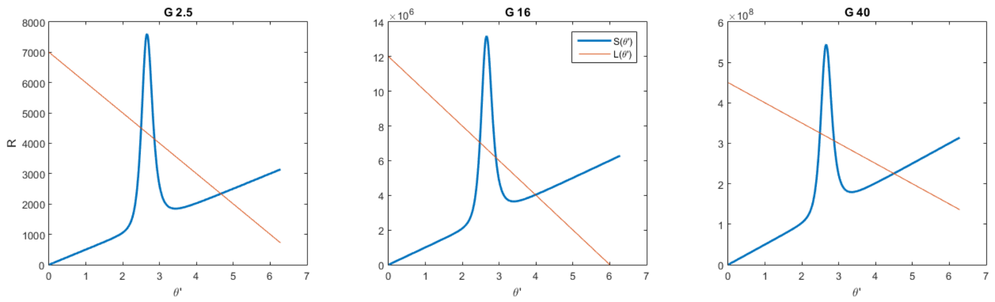

Figure 5. Energy and Characteristic Curves of the Systems for G 2.5, 16 and 40.

5 RESULTS AND DISCUSSION

Solving the system of equations presented in (6), it is possible to obtain the results showed on Figs. 6, 7, 8 and 9 for the three cases of balance quality degree.

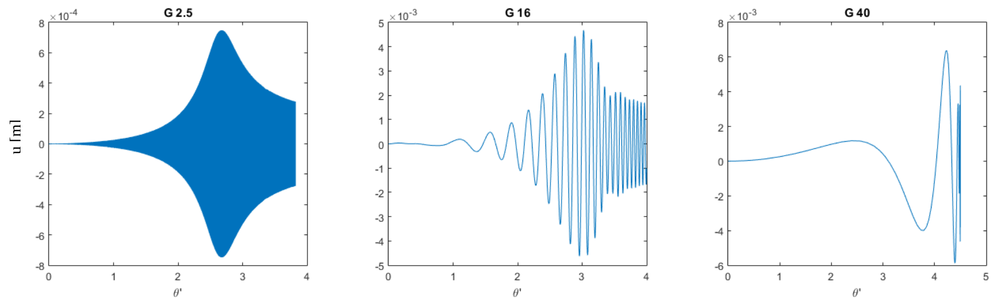

Figure 6. Displacement vs. Frequency of power supply.

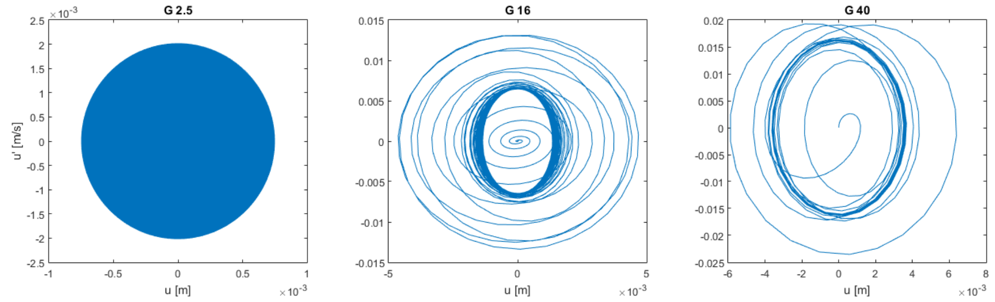

Figure 7. Phase portrait for the three cases.

Proceedings of the XXXVIII Iberian Latin-American Congress on Computational Methods in Engineering
P.O. Faria, R.H. Lopez, L.F.F. Miguel, W.J.S. Gomes, M. Noronha (Editores), ABMEC, Florianópolis, SC, Brazil, November 5-8, 2017.

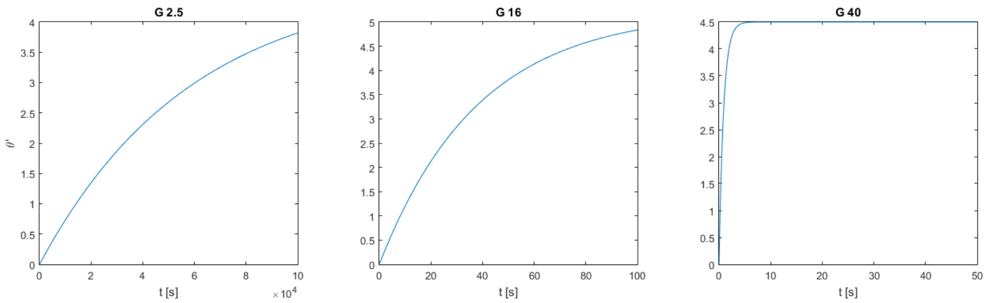

Figure 8. Frequency vs. time.

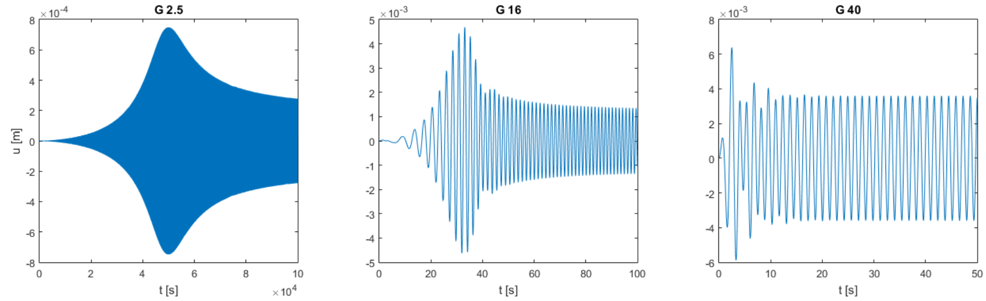

Figure 9. Displacement vs. time

First, comparing the obtained displacement charts in Fig. 9 against the oscillograms of direct transition from Kononenko (1969), it is possible to notice the similarities, as both begin with a small displacement, followed by a peak and then they go to a steady state considerably higher than the beginning but smaller than the peak.

When analyzing Fig. 6, it is possible to see that for G2.5 the peak of displacement occurs at the natural frequency of the structure, as one would expect from an ideal system. However, the displacement for G16 and G40 happen at higher frequencies than the natural frequency of the system, which is a characteristic of non-ideal behavior like the Sommerfeld effect. One should watch-out, when looking at G40, that, as predicted by Fig. 5, at around the frequency of 4.5 rad/s the power supply cannot provide enough energy for the system to continue its motion, which leads to a steady point, at around 5s, as can be observed in Figure 8.

When looking at the Phase Portraits in Fig. 7 it is even clearer that for the cases of G16 and G40 the behavior of the system is non-ideal, characterized by the oval shaped steady state (the denser lines in the figures), resembling the study of Simons (2008) and Silva (2012). While G16 and G40 present a non-ideal behavior, for the case of G2.5 this behavior is absent, much probably linked to its very small eccentricity, making the impacts of the non-ideal behavior unnoticed.

Another point that can be pointed out is the time needed for the system to accelerate its rotor (angular acceleration) is much higher when the quality of balance is lower, i.e. the eccentricity is lower. This is related to the power supply needing to provide smaller energy quantity in order to observe the non-ideal phenomena, and therefore reducing the structure available power to accelerate its rotor.

6 CONCLUSION

As it was observed, the quality of balance degree affects highly the response of the system and its chance to present non-ideal behaviors. For the G2.5, which is the ISO 1940/1 regulation for wind turbine, the non-ideal behavior cannot be noticed at all. However, if this is increase to a G16, then the non-ideal behaviour, in this study the Sommerfeld effect, starts to be visible, and it can bring structural impacts on the system, especially because this behavior offset the point of maximum displacement of the tower from its natural frequency, which can be dangerous for the structure given that most designs are made considering ideal behaviors and maximum displacements in the natural frequency point of the system.

Therefore, from the data provided in this study, it is extremely important for the wind turbines to present low and inside regulations eccentricity values in order to avoid critical structural consequences.

As the power supply used in this study can vary for several different tower heights and configurations, a recommendation for future studies would be to understand how the height and material of the tower, together with the quality of balance, could influence and/or aggravate non-ideal behaviors.

ACKNOWLEDGMENTS

The authors acknowledge support by FAPESP, CAPES and CNPq, all Brazilian research funding agencies.

REFERENCES

KONONEKO, V. O. *Vibrating systems with a limited power supply*. Londres, Iliffe Books Ltda, 1969. 231p.

SIMONS, G. K. E. *Uma Investigação sobre a aplicabilidade da Teoria de Sistemas Não-Ideais a fundações de Máquinas Reais*. Master Thesis, Escola Politécnica da Universidade de São Paulo, São Paulo, 2008.

QUILLIGAN, A.; O'CONNOR, A.; PAKRASHI, V. *Fragility analysis of steel and concrete wind turbine towers*. Engineering Structures: Elsevier Journal, 36 (2012), 270-282.

SILVA, H. F. *Análise do comportamento dinâmico não-linear de Estruturas sob Excitação de suportes não ideal*. PhD Thesis, Escola Politécnica da Universidade de São Paulo, São Paulo, 2012.